Clinical & Translational Immunology

Australian and New Zealand Society for Immunology Inc.

Clinical & Translational Immunology 2022; e1361. doi: 10.1002/cti2.1361
www.wileyonlinelibrary.com/journal/cti

ORIGINAL ARTICLE

DROSHA but not DICER is required for human haematopoietic stem cell function

Karen Gu[1,2†], Carina Walpole[3†], Shayarana Gooneratne[1†], Xin Liu[1], Oscar L Haigh[3], Kristen J Radford[3‡] & Mark MW Chong[1,2‡]

[1]St Vincent's Institute of Medical Research, Fitzroy, VIC 3065, Australia
[2]Department of Medicine (St Vincent's), University of Melbourne, Fitzroy, VIC 3065, Australia
[3]Mater Research Institute, Translational Research Institute, The University of Queensland, Woolloongabba, QLD 4102, Australia

Correspondence
MMW Chong, St Vincent's Institute of Medical Research, 9 Princes Street, Fitzroy, VIC 3065, Australia.
E-mail: mchong@svi.edu.au

KJ Radford, Mater Research Institute, Translational Research Institute, The University of Queensland, 37 Kent Street, Woolloongabba, 4102, QLD Australia.
E-mail: kristen.radford@mater.uq.edu.au

[†]Equal contributors.
[‡]Equal contributors.

Received 25 July 2021;
Revised 18 November 2021;
Accepted 27 November 2021

doi: 10.1002/cti2.1361

Clinical & Translational Immunology
2022; **11**: e1361

Abstract

Objectives. DROSHA and DICER have central roles in the biogenesis of microRNAs (miRNAs). However, we previously showed that in the murine system, DROSHA has an alternate function where it directly recognises and cleaves protein-coding messenger (m)RNAs and this is critical for safeguarding the pluripotency of haematopoietic stem cells (HSCs). Maintenance of murine HSC function is dependent on DROSHA-mediated cleavage of two mRNAs, *Myl9* and *Todr1*. The goal of this study is to determine whether this pathway is conserved in human HSCs. **Methods.** DROSHA and DICER were knocked down in human cord blood $CD34^+$ HSCs with short hairpin RNAs. The function of HSCs was analysed *in vitro* and in humanised mice. Analysis of mRNA cleavage was performed by capture of 5′ phosphorylated RNAs. **Results.** Consistent with murine HSCs, DROSHA knockdown impaired the differentiation of human HSCs *in vitro* and engraftment into humanised mice, whereas DICER knockdown had no impact. DROSHA cleaves the MYL9 mRNA in human HSCs and DROSHA deficiency resulted in the accumulation of the mRNA. However, ectopic expression of MYL9 did not impair human HSC function. We were unable to identify a human homolog of Todr1. **Conclusion.** A miRNA-independent function of DROSHA is critical for the function of human HSCs. DROSHA directly recognises and degrades mRNAs in humans HSCs. However, unlike in murine HSCs, the degradation of the MYL9 mRNA alone is not critical for human HSC function. Therefore, DROSHA must be inhibiting other targets and/or has another miRNA-independent function that is essential for safeguarding the pluripotency of human HSCs.

Keywords: DICER, DROSHA, haematopoietic stem cells, microRNA, mRNA

INTRODUCTION

The differentiation of haematopoietic stem cells (HSCs) into the range of immune and blood cell types is a highly regulated process and involves a series of lineage branch point decisions. Haematopoiesis bifurcates at an early stage via the common myeloid and lymphoid progenitors (CMP and CLP).[1,2] CMPs give rise to granulocytes, monocytes, dendritic cell (DC) and other myeloid lineages, while CLPs give rise to T cells, B cells and innate lymphocytes.

Haematopoietic stem cells and other early progenitors have been assumed to be multipotent, and it is thought that as these progenitors differentiate along a particular lineage pathway, their transcriptional programs are progressively fixed and the potential to differentiate into other lineages is lost. While there is ample evidence to support this concept, there is also evidence that lineage decisions may actually be fixed or imprinted at much earlier stages. Fate mapping in mice found that early progenitors are already biased towards lymphoid, myeloid and/or DC lineages.[3] We previously showed that murine HSCs actively transcribe two genes, *Myl9* and *Todr1*, that inhibit their ability to differentiate into myeloid lineages.[4] However, the *Myl9* and *Todr1* messenger (m)RNAs are actively degraded by the RNase III enzyme DROSHA. In the absence of DROSHA, expression of these two mRNAs is permitted and the ability of HSCs to differentiate is impaired.

DROSHA is best known for its role in the biogenesis of microRNAs (miRNAs). It functions early in the biogenesis pathway where it processes stem-loop containing primary (pri)-miRNA transcripts.[5] This releases a stem-loop intermediate that is further processed by another RNase III enzyme, DICER, to produce the mature miRNA.[6] Early studies from our laboratory and others comparing the impact of DROSHA and DICER deficiency in various murine tissues suggested that the only function of these enzymes is in the biogenesis of miRNAs.[7] However, in HSCs, it is the degradation of target mRNAs that is critical. DROSHA directly inhibits specific mRNAs, such as *Myl9* and *Todr1*, by recognising and cleaving stem-loop structures within these transcripts. A similar requirement for this mRNA cleavage function of DROSHA was also found in murine neural[8] and embryonic stem cells.[9] In fact, DROSHA-mediated mRNA cleavage appears to be largely unique to stem cells, at least in the mouse. The one exception is cleavage of the *Dgcr8* mRNA, which has been reported in a range of cell types.[10,11] The DGCR8 protein is a core component of the DROSHA complex, and thus, this cleavage of the *Dgcr8* mRNA is thought to serve as a mechanism to autoregulate the DROSHA complex.[10] DROSHA is expressed in all cell types, where it is required for miRNA biogenesis. This restriction of only its mRNA cleavage function suggests that DROSHA must be highly regulated.

While it clear that DROSHA-mediated mRNA cleavage is critical for the differentiation of murine HSCs, whether this is an evolutionary conserved requirement is unknown. In this study, we investigate whether this requirement is conserved in humans by analysing the impact of knocking down DROSHA and DICER in human HSCs.

RESULTS

Knockdown of DROSHA or DICER in human cord blood CD34$^+$ HSCs impairs miRNA expression

To investigate the requirement of the miRNA biogenesis pathway enzymes DROSHA and DICER in human HSCs, we constructed two different lentiviral short hairpin (sh)RNA constructs to knockdown each gene in CD34$^+$ cells purified from cord blood. We chose DROSHA shRNA #1, which resulted in $\sim$80% mRNA knockdown (Figure 1a), and DICER shRNA #2, which resulted in $\sim$70% mRNA knockdown (Figure 1b), for subsequent analyses. We also checked that these shRNAs downregulated DROSHA and DICER protein in Jurkat cells (Supplementary figure 1). Knockdown of either DROSHA or DICER impaired the expression of miR-17-5p (Figure 1c) in HSCs, a miRNA that is highly expressed throughout the haematopoietic system.[12] This suggests that both constructs are equally effective at ablating the miRNA biogenesis pathway.

Knockdown of DROSHA but not DICER impairs differentiation of CD34$^+$ HSCs *in vitro*

Following transduction, the GFP$^+$ shRNA-expressing HSCs were sorted and returned to X-VIVO-15 to expand for a further 3 days. After this expansion, there was no discernible difference

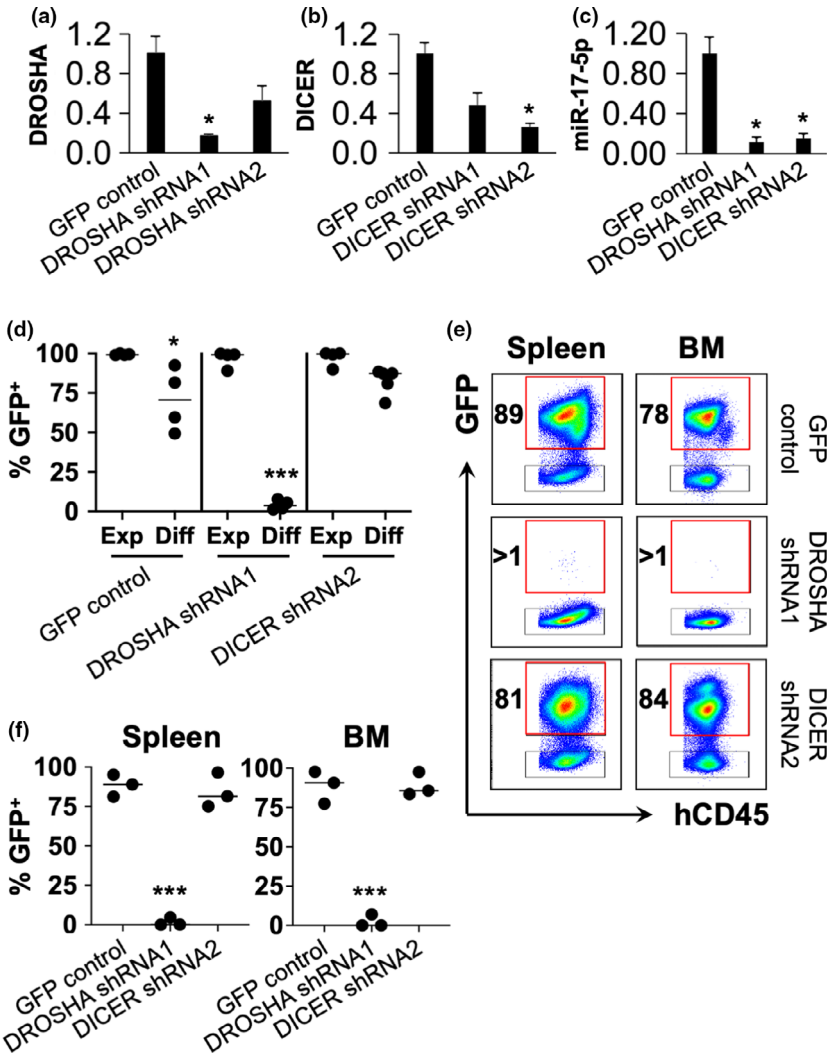

Figure 1. Knockdown of DROSHA, but not DICER, in human HSCs impairs engraftment into humanised mice. Lentiviral shRNAs against **(a)** DROSHA or **(b)** DICER (two different target sequences each) were transduced into CD34$^+$ cord blood HSCs. Cells transduced with the empty vector were analysed as controls. The transduced cells (GFP$^+$) were sorted 3 days later and analysed by quantitative RT-PCR for the expression of DROSHA or DICER, normalised to GAPDH. The mean ± SEM of four replicates performed over two separate experiments is shown. *$P < 0.05$ compared to empty GFP. **(c)** The same cells were also analysed for expression of miR-17-5p, relative to U6 snRNA, by quantitative TaqMan RT-PCR. * $P < 0.05$ compared to empty GFP. **(d)** Lentiviral shRNA-transduced CD34$^+$ cells were sorted on GFP. The purified GFP$^+$ cells were then expanded in X-VIVO-15 for 3 days followed by culture in DC differentiation medium for a further 12 days. The cultures were analysed for the percentage of GFP$^+$ cells by flow cytometry after the 3-day expansion (Exp) and after the 12-day differentiation culture (Diff). Data from four replicates for each condition performed over four separate experiments are shown. Each dot is of an individual experiment. *$P < 0.05$, ***$P < 0.0005$ compared to after 3 days of expansion. **(e)** shRNA-transduced CD34$^+$ cells sorted on GFP and were transplanted into 5-day-old NSG-SGM3 pups. After 9 weeks, the human haematopoietic compartment (hCD45$^+$) of the bone marrow and spleen was analysed for the percentage of GFP$^+$ cells by flow cytometry. A representative set of flow cytometric plots is shown. **(f)** Data are shown from three animals for each group. Each dot is an individual animal engrafted with an independent HSC transduction. The means are also indicated. ***$P < 0.0005$ compared to mice engrafted with GFP only control HSCs.

between the DROSHA knockdown, DICER knockdown or control (GFP only lentivirus) cultures, with almost all cells remaining GFP$^+$ across the cultures. There was also little difference in cell cycle status between the three cultures (Supplementary figure 2). The cells were then transferred into DC differentiation cultures for 12 days. After this differentiation, very few GFP$^+$ cells remained in the DROSHA knockdown cultures, whereas the majority of cells in the DICER knockdown and empty vector control cultures remained GFP$^+$ (Figure 1d). No difference

in the frequency of $CD11c^+$ or $CLEC9A^+$ DC populations was found between the DICER knockdown and control cultures (not shown). The loss of GFP^+ cells in the DROSHA knockdown cultures means that there is either silencing of the transduced lentivirus or outgrowth of untransduced cells. Either way, this suggests that DROSHA deficiency but not DICER deficiency impairs the differentiation, proliferation or survival of human $CD34^+$ cells *in vitro*, under DC differentiating conditions.

Knockdown of DROSHA but not DICER in $CD34^+$ HSCs impairs engraftment into humanised mice

We next investigated whether the HSCs with knockdown of DROSHA or DICER engraft into humanised mice. Following transduction of the $CD34^+$ cells *in vitro*, the cells were sorted on GFP (Supplementary figure 3) and injected into 5-day-old NSG-SGM3 pups to produce humanised mice. After 9 weeks, the mice were analysed for the presence of GFP^+ versus GFP^- $hCD45^+$ cells. Consistent with the *in vitro* cultures, we observed robust engraftment of DICER knockdown or GFP only control cells in these mice but poor engraftment of DROSHA knockdown cells (Figure 1e and f). This differential impact of DROSHA and DICER deficiency in human $CD34^+$ HSCs mirrors the differential impact of DROSHA and DICER deficiency that we previously observed in murine HSCs.[4] Given that knockdown of either DROSHA or DICER impairs miRNA expression (Figure 1c), this implies that it is a miRNA-independent function of DROSHA that is critical for HSC function.

Because human HSCs with DICER knockdown still engrafted into humanised mice, we could determine whether impaired miRNA biogenesis affected haematopoiesis. Analysis of the GFP^+ compartment of mice grafted with DICER knockdown HSCs (Supplementary figure 4) revealed little difference in the frequency of dendritic cell, monocyte, B-cell or T-cell populations compared to mice engrafted with GFP only control HSCs (Figure 2).

DROSHA cleaves the MYL9 mRNA at multiple locations

We previously showed that DROSHA deficiency impairs the differentiation of murine HSCs primarily because of the upregulation of two genes, *Myl9* and a previously undescribed gene designated *2610318N02Rik* that we named Target of DROSHA 1 (*Todr1*).[4] Knockdown of DROSHA indeed resulted in the upregulation of *MYL9* in human $CD34^+$ HSCs, whereas expression was unchanged in cells with DICER knockdown (Figure 3a).

The 5′ untranslated regions (UTRs) and open reading frames in the mouse and human *MYL9* mRNAs are highly conserved, with 86% identity, and the protein sequence differs by only a single amino acid. Their 3′UTRs, however, share little homology. We showed that in murine HSCs, DROSHA recognises and cleaves a stem-loop structure near the start of the open reading frame of the *Myl9* mRNA.[4] This direct recognition of an mRNA target is independent of miRNAs and was found to be essential for maintaining the pluripotency of murine HSCs. We therefore investigated whether the human *MYL9* mRNA is also subject to cleavage in human HSCs.

Endonucleolytic cleavage of an mRNA leaves a 5′-monophosphate remnant, and this can be captured with RNA ligase.[9] To map potential cleavage sites in the *MYL9* mRNA, an oligonucleotide adaptor was ligated to $polyA^+$ RNA extracted from human $CD34^+$ cells (ligation only occurs if the RNA contains the 5′-monophosphate). PCR was then performed using a forward primer in the adaptor sequence together with a series of reverse primers along the length of the *MYL9* open reading frame. Sequencing of the resulting PCR products identified one cleavage site in the 5′ UTR and four within the open reading frame of the *MYL9* mRNA (Figure 3b). However, none of these corresponded to the cleavage site that was previously identified in the murine *Myl9* transcript. Analysis of the sequence immediately upstream of the five cleavage sites with RNAfold[13] predicts that the RNA folds into secondary stem-loop structures (Figure 3c) that are likely to be directly recognised by DROSHA.

To confirm that DROSHA cleaves the human *MYL9* mRNA, $CD34^+$ cells with DROSHA knockdown were analysed for adaptor ligation to $polyA^+$ RNA. Ligation, and therefore cleavage, was measured by quantitative PCR using a forward primer in the adaptor sequence and a reverse primer specific for the position 324 cleavage site. DROSHA knockdown was found to reduce cleavage of the *MYL9* mRNA to approximately 40% of control cells (Figure 3d), confirming that DROSHA-mediated cleavage of the *MYL9* mRNA does occur in human HSCs.

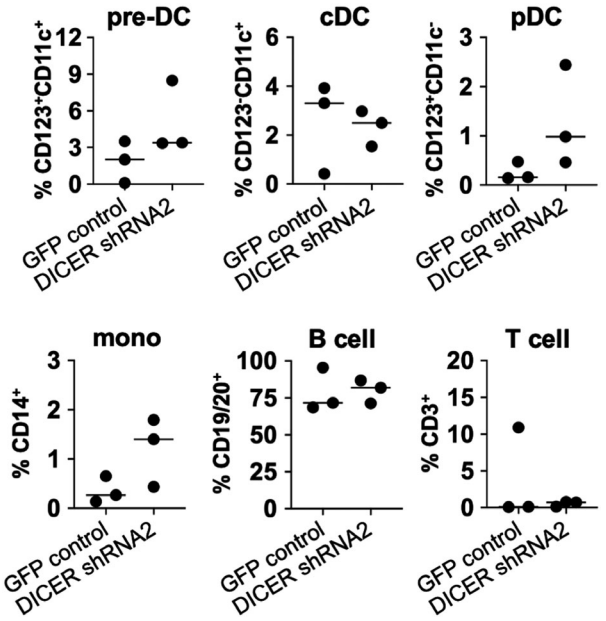

Figure 2. Humanised mice engrafted with DICER knockdown human HSCs do not exhibit significant abnormalities in haematopoietic populations. The hCD45$^+$GFP$^+$ compartment (derived from DICER shRNA or GFP only transduced CD34$^+$ cells) of the spleen was analysed for the frequency of the indicated haematopoietic populations 9 weeks after engraftment. Data are shown from three animals for each group. Each dot is an individual animal engrafted with an independent HSC transduction. The means are also indicated. pre-DC, pre-dendritic cells; cDC, conventional dendritic cells; pDC, plasmacytoid dendritic cell; mono, monocyte.

The human genome does not encode a homolog of the murine *Todr1* gene

The *Todr1* mRNA is another target of DROSHA in murine HSCs and cleavage of *Todr1* is also necessary for maintaining the pluripotency of these cells.[4] The murine *Todr1* gene (also known as *2610318N02Rik)* is located on chromosome 16 between the *Sdf2l1* and *Ppil2* genes. This gene contains a 918nt open reading frame that is predicted to encode a 34 kDa protein, and we showed that this open reading frame indeed encodes a protein that impairs murine HSC function.[4] This gene, however, does not appear to be conserved in humans. A gene, *TCONS_l2_00017631*, is annotated between *SDF2L1* and *PPIL2* in the syntenic region on human chromosome 22. Murine *Todr1* is expressed by a range of stem cell types, including embryonic stem cell and HSCs (not shown). Analysis of an RNAseq dataset and a ChIPseq dataset from human embryonic stem cells confirms that there is transcription of this locus in human cells (Figure 4a). *TCONS_l2_00017631* appears to contain a 331nt open reading frame that is predicted to encode a 12.4 kD protein (Figure 4b), but this sequence is unlike the TODR1 protein. We could not detect an upregulation of the *TCONS_l2_00017631* mRNA in human CD34$^+$ HSCs following DROSHA knockdown (Figure 4c). Thus, we do not believe that there is a human equivalent of the murine *Todr1* gene.

Impact of MYL9 overexpression on HSC function

If the impact of DROSHA deficiency on the function of human HSCs is because of the loss of *MYL9* mRNA cleavage, then ectopic expression of MYL9 in HSCs might be expected to at least partially phenocopy DROSHA knockdown. To investigate this, HSCs were transduced with a lentiviral MYL9-IRES-GFP construct then engrafted into 5-day-old NSG-SGM3 pups to produce humanised mice. HSCs with ectopic MYL9 expression engrafted as well as cells transduced with only GFP (Figure 5a). This indicates that expression of MYL9 does not impair the proliferation or survival of HSCs. We also observed little difference in the frequency of dendritic cell, monocyte, B-cell or T-cell populations within GFP$^+$ hCD45$^+$ compartment of mice engrafted MYL9-IRES-GFP or GFP only HSCs (Figure 5b). Thus, the upregulation of MYL9 in HSCs alone is not sufficient to phenocopy the impact of DROSHA deficiency.

DISCUSSION

We have shown that DROSHA is absolutely critical for the function of human CD34$^+$ HSCs, whereas DICER is not. Because both DROSHA and DICER deficiency impaired the expression of miRNAs in these cells, it suggests that the miRNA pathway is not essential, at least for the engraftment of human HSCs into humanised mice. This also suggests that it is a miRNA-independent function of DROSHA that is critical.

We previously showed that in murine HSCs it is the direct recognition and cleavage of two mRNAs, *Myl9* and *Todr1*, by DROSHA that is critical for maintaining the pluripotency of these cells.[4] However, while DROSHA-mediated cleavage of the human *MYL9* mRNA does indeed occur in human HSCs, inhibition of MYL9 expression is not

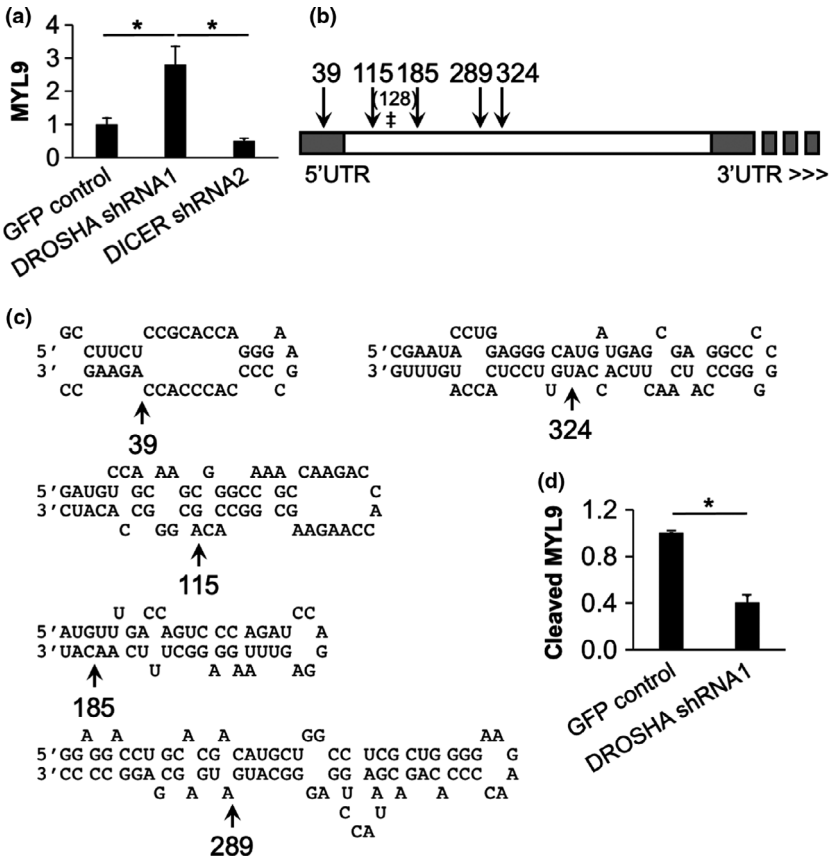

Figure 3. The *MYL9* mRNA is directly cleaved by DROSHA in human HSCs. **(a)** $CD34^+$ cells were transduced with lentiviral shRNAs against DROSHA or DICER. Three days later, total RNA was extracted and the expression of MYL9 was measured by quantitative PT-PCR, normalised to GAPDH. The mean ± SEM of six replicates performed over two separate experiments is shown. *$P < 0.05$ compared to the GFP only control. **(b)** Cleavage of the MYL9 mRNA was detected by ligating an RNA oligonucleotide adaptor to $polyA^+$ RNA purified from $CD34^+$ cells. Only RNAs with a 5′ monophosphate, a hallmark of endonucleolytic cleavage, will be ligated. PCR was then performed with one primer in the adaptor and one in *MYL9*. Sequencing of the resulting PCR products identified cleavage sites within *MYL9*. The cleavage site previously identified in *Myl9* from mouse HSCs is indicated by ‡. **(c)** The RNA sequence surrounding the human *MYL9* cleavage sites is predicted to fold into stem-loop structures. **(d)** Knockdown of DROSHA in human $CD34^+$ cells impairs MYL9 cleavage. A quantitative RT-PCR measuring RNA adaptor ligation to the position 324 cleavage site in MYL9, normalised to total GAPDH is shown. The mean ± SEM of four replicates performed over two separate experiments is shown. *$P < 0.05$ compared to GFP only control.

essential for maintaining the function of these cells because overexpression of MYL9 in cord blood $CD34^+$ HSCs did not prevent their engraftment into humanised mice. Moreover, we were unable to identify the human equivalent of the *TODR1* gene. Thus, the requirement of this cleavage mechanism, as least of the *Myl9* and *Todr1* mRNAs, does not appear to be conserved between human and mouse.

An interesting finding was that the *MYL9* mRNA is cleaved at multiple locations in human HSCs, with five cleavage sites identified. While all these sites are predicted to fold into secondary stem-loop structures, it is unlikely that all five stem-loops will be present at the same time because of steric constraints of the structures being in such close proximity to each other. This suggests that these stem-loops may not be very stable and that DROSHA may not be targeting the *MYL9* mRNA with much efficiency. This is in contrast to the murine *Myl9* mRNA, which we previously showed to be efficiently cleaved at a single position in murine HSCs by DROSHA.[4] This differential cleavage of the human *MYL9* and murine *Myl9* mRNAs suggests that the two may be under different constraints. In the case of murine *Myl9*, inhibition of expression is critical for maintaining murine HSC function.

While cleavage of the *MYL9* mRNA alone is not essential for human HSC function, it is clear that a

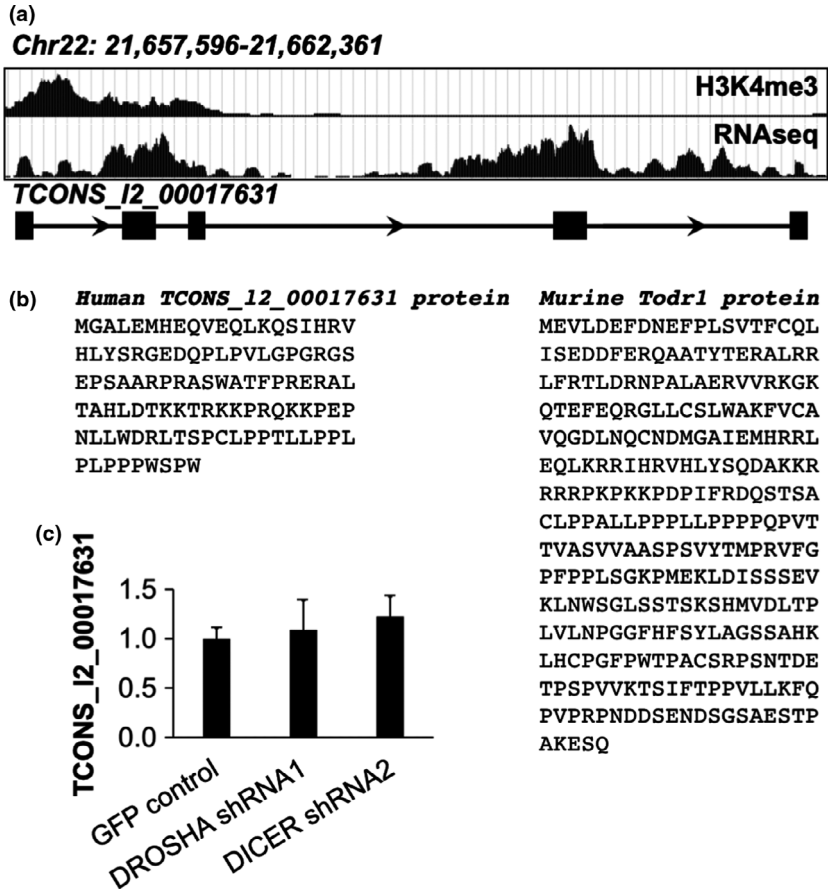

Figure 4. Todr1 does not appear to be conserved in humans. **(a)** The syntenic region of the murine *Todr1* locus is located on human chromosome 22, which contains the gene *TCONS_l2_00017631*. An alignment of a RNAseq and a H3K4me3 ChIPseq dataset from human embryonic stem cells is shown. **(b)** Comparison of the protein sequence of the predicted open reading frame in human *TCONS_l2_00017631* with the protein sequence of murine TODR1. **(c)** $CD34^{+}$ cells were transduced with lentiviral shRNAs against DROSHA or DICER. Three days later, total RNA was extracted and the expression of *TCONS_l2_00017631*, relative to GAPDH, was measured by quantitative PT-PCR. The mean ± SEM of four replicates performed over two separate experiments is shown.

non-miRNA function of DROSHA is critical. It is possible that DROSHA's mRNA cleavage function is important, but it is inhibition of different target that is required for maintaining HSC function. It could also be that HSC impairment caused by DROSHA deficiency involves the upregulation of multiple targets, not just MYL9, and thus, overexpressing MYL9 alone does not affect HSC function.

While studies in gene knockout mice suggest that mRNA cleavage is the other significant function of DROSHA,[14] other miRNA-independent functions could be playing a role in human HSCs. DROSHA was originally identified as an enzyme involved in pre-ribosomal processing.[15] However, there has been little evidence from gene knockout studies to support such a function in either mouse or human cells.[5,16] One possible exception may be human mesenchymal stem cells, in which knockdown of DROSHA appears to result in reduced ribosomal RNA levels and impaired cell proliferation.[17]

DROSHA could potentially be regulating gene expression in HSCs by influencing alternative mRNA splicing. When binding to stem-loop structures close to splice sites in primary RNA transcripts, DROSHA can promote exon skipping, although only a handful of examples have been reported.[18,19] It remains unknown whether this function of DROSHA has widespread impacts on the transcriptional landscape of a cell.

The biogenesis of another class of small RNAs, known as DNA-damage-induced small RNAs, is also dependent on DROSHA and DICER.[20] Unlike miRNAs that form a complex with Argonaute proteins to target protein-coding mRNAs,[21]

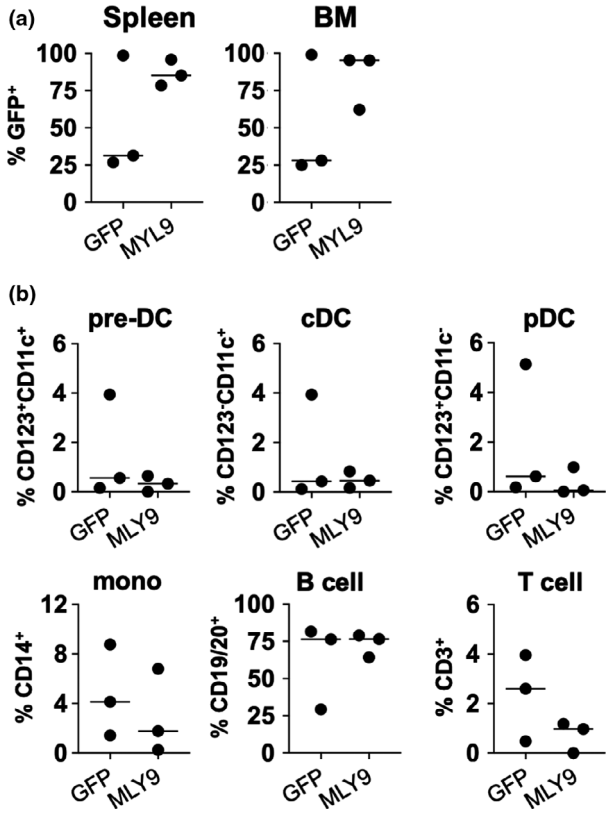

Figure 5. MYL9 overexpression does not impair the engraftment of human HSCs into humanised mice. **(a)** MYL9-IRES-GFP or GFP only transduced $CD34^+$ cells were sorted on GFP and transplanted into 5-day-old NSG-SGM3 pups. After 9 weeks, the human haematopoietic compartment ($hCD45^+$) of the bone marrow and spleen was analysed for the percentage of GFP^+ cells by flow cytometry. Data are shown from three animals for each group. Each dot is an individual animal engrafted with an independent HSC transduction. The means are also indicated. **(b)** The $hCD45^+GFP^+$ compartment (derived from MYL9-IRES-GFP or GFP only transduced $CD34^+$ cells) of the spleen of the same animals was analysed for the frequency of the indicated haematopoietic populations. pre-DC, pre-dendritic cells; cDC, conventional dendritic cells; pDC, plasmacytoid dendritic cell; mono, monocyte.

DNA-damage-induced small RNAs localise to double-stranded DNA breaks and are required for the formation of DNA-damage response foci and the repair of those breaks.[20,22] DROSHA deficiency could potentially be impairing HSC function by causing genome instability.

Clearly, further analysis is required to determine precisely how DROSHA deficiency impairs human HSC function. It is possible that one of these other miRNA-independent functions is responsible, or a combination of these. Understanding the impact of DROSHA abnormalities in different cellular contexts will be important as mutations in the gene encoding DROSHA are increasingly being reported in a range of diseases, especially cancer.[23–27] The assumption has been that DROSHA mutations are affecting miRNA expression and that perturbations in specific miRNAs must be contributing to disease pathogenesis. The present study therefore highlights the importance understanding the function of DROSHA in each cell type because the influence of such mutations could in fact be independent of miRNAs.

METHODS

Lentiviral vectors

shRNA-mediated knockdown of target genes was achieved with the pLKO.1GFP lentiviral vector.[28] The sequences GAGGAAGCCAAGCAGTTATTT (#1) and CGAAGCTCTTTGGTG AATAAT (#2) in *DROSHA* were targeted, while the sequences CCGCATGGTGGTGTCAATATT (#1) and CCTTCATGGAT AGTCTTTAAT (#2) in *DICER1* were targeted.

An hMYL9-IRES-eGFP expression lentivirus was generated by PCR amplification of the human *MYL9* open reading frame from Jurkat cell RNA. This was ligated to an IRES-GFP cassette and inserted into an empty HIV lentiviral backbone. The IRES-GFP cassette alone was inserted into the lentivirus as a control.

Lentiviruses for *DROSHA or DICER1* knockdown or overexpression of MYL9 and controls were generated by cotransfection of each plasmid with the lentiviral packaging plasmids pVSVg (envelope), pMDLg/pRRE (gag/pol) and pRSV.rev into HEK293T cells. Supernatants were collected and concentrated by ultracentrifugation at 70 000 *g* for 2 h at 4°C. The viral pellets were resuspended in PBS and stored at −80°C in single-use aliquots. Viral stocks were titred before use.

Preparation of human HSCs for lentiviral transductions

Umbilical cord blood was obtained from the Queensland Cord Blood Bank following written informed consent (Mater Adult Hospital Human Ethics Committee, HREC/13/MHS/83). Cord blood-derived $CD34^+$ HSCs were isolated by MACS sorting (Miltenyi Biotec, Bergisch Gladbach, Germany) and cryopreserved before use as previously described.[29] When required for transductions, the $CD34^+$ cells were thawed and rested overnight in X-VIVO-15 (Lonza, Basel), 10% FCS, 50 ng mL^{-1} human FLT3L, 50 ng mL^{-1} human SCF, 20 ng mL^{-1} human IL-3 and 50 ng mL^{-1} human TPO (all cytokines from Peprotech, Cranbury) at 4×10^6 cells mL^{-1}. Cells for humanised mice were thawed on the day the recipient pups were born. Wells of a 96-well plate were pre-coated with 1ug Retronectin (Scientifix, Clayton) in 50 μL HBSS (Thermo Fisher Scientific, Waltham) overnight at 4°C, blocked with 2% human serum albumin (CSL Behring Australia, Broadmeadows) in HBSS and washed twice with X-VIVO-15. The cells were seeded at 2×10^5 per well and transduced with lentivirus at an MOI of 2.5 in 100 μL per

well of the X-VIVO-15/FCS/cytokine. After 72 h, the cells were sorted on GFP on a Moflo Astrios (Beckman Coulter, Brea) or FACSAria Fusion (BD Biosciences, Franklin Lakes) for analysis *in vitro* or the generation of humanised mice.

In vitro differentiation of dendritic cells

Sorted GFP$^+$CD34$^+$ HSCs were allowed to expand for a further 72 h in X-VIVO-15/FCS/cytokine media at 2.5×10^4 mL^{-1} before differentiation into DCs according to a modified published protocol.[30] In brief, the expanded cells were cultured at a density of 6.25×10^4 mL^{-1} in RPMI 1640, 10% FCS, 1 mM HEPES, 1 mM sodium pyruvate, 100 U mL^{-1} penicillin-streptomycin, 2 mM Glutamax (all Thermo Fisher Scientific) and 50 μM β-mercaptoethanol (Sigma-Aldrich, St Louis, MO, USA) supplemented with 100 ng mL^{-1} human FLT3L, 20 ng mL^{-1} human SCF, 2.5 ng mL^{-1} human IL-4, 2.5 ng mL^{-1} human GM-CSF (all cytokines from Peprotech) and 1 μM StemRegenin 1 (STEMCELL Technologies, Vancouver). Media and cytokines were replenished on Day 6 of the differentiation culture and harvested for analysis by flow cytometry after 12 days.

Generation of humanised mice

NOD.Cg-*Prkdc*^{scid} *Il2rg*^{tm1Wjl} Tg(CMV-IL-3, CSF2, KITLG)1Eav/MloySzJ (referred to as NSG-SGM3 mice) were originally generated at the Jackson Laboratory, and a breeding colony was established at the Translational Research Institute. All experiments were approved by the University of Queensland Animal Ethics Committee.

The 5-day-old NSG-SGM3 pups were subjected to 100 cGy γ-irradiation immediately prior to intrahepatic injection of $1–3 \times 10^5$ GFP-sorted CD34$^+$ HSCs in HBSS. After 8 weeks, the mice were bled to confirm reconstitution of human haematopoietic cells by flow cytometric analysis for mouse versus human CD45. The spleen and bone marrow of mice with adequate engraftment were analysed at 9 weeks post-transplantation.

The spleens were prepared by cutting into small fragments and digesting with 35 U mL^{-1} type IV collagenase (Worthington Biochemical, Lakewood) and 1.4 mg mL^{-1} DNase I (Sigma-Aldrich) in RPMI 1640, 10% FCS, 1 mM HEPES, 1 mM sodium pyruvate, 100 U mL^{-1} penicillin-streptomycin, 2 mM Glutamax, 1× NEAA (all Thermo Fisher Scientific) and 50 μM β-mercaptoethanol (Sigma-Aldrich). The cell suspension was then filtered through a 40-μM cell strainer and purified on 1.077g cm^{-3} Percoll (GE Healthcare, Chicago, USA) centrifuged at 1700 *g* for 10 min. Bone marrow was harvested by flushing the long bones with MACS Buffer (Miltenyi Biotec) and passing through a 40-μM cell strainer to remove any bone fragments.

Flow cytometry was performed on a LSRII Fortessa (BD Biosciences) using the antibodies listed in Supplementary table 1 and analysed on Flowjo ver10.

Mapping cleavage sites in the MLY9 mRNA

Mapping of exonucleolytic cleavage site in the *MYL9* transcript was performed essentially as described previously.[4] In brief, PolyA$^+$ RNA was extracted from purified CD34$^+$ cord blood HSCs using Oligo(dT)$_{25}$ Dynabeads (Thermo Fisher Scientific). One μg of the purified RNA was then incubated with a 5′-CACGACGCUCUUCCGAUCU RNA oligonucleotide adaptor and T4 RNA ligase 1 (New England Biolabs, Ipswich, USA). This results in a ligation of the adaptor to any RNAs with a 5′ phosphate, a hallmark of endonucleolytic cleavage. The reaction was then repurified on the Oligo(dT)$_{25}$ beads to remove excess adaptor and reverse transcribed with random hexamers and Superscript III (Thermo Fisher Scientific). Tiled PCRs were then performed using the 5′ adaptor primer in combination with the reverse primers MYL9-213, MYL9-257, MYL9 372 or MYL9r, which are spaced at regular interval in the *MYL9* mRNA (Supplementary table 2). The resulting PCR products were Sanger sequenced to determine the adaptor-*MYL9* ligation point and therefore the original cleavage site.

Quantitative PCR analyses for mRNA and miRNA expression

Total RNA was extracted from $\sim 10^5$ GFP$^+$ CD34$^+$ cells using Trizol (Thermo Fisher Scientific) and Pink Co-precipitant (Meridian Bioscience, London) as a carrier. Half the RNA was reversed transcribed with Superscript III, and one-tenth of the resulting cDNA was then analysed by quantitative PCR using GoTaq qPCR Master Mix (Promega, Madison). The primer pairs to measure target genes are listed in Supplementary table 2. For the measurement of miR-17-5p or U6 snRNA expression, one-tenth of the total RNA was used directly in TaqMan MicroRNA Assays (Thermo Fisher Scientific) according to the manufacturer's protocol.

Nested quantitative PCR analyses for mRNA cleavage

PolyA$^+$ RNA was extracted from $\sim 2 \times 10^4$ GFP$^+$ CD34$^+$ cells using Oligo(dT)$_{25}$ Dynabeads, with a slight modification of the manufacturer's protocol. After the final wash, instead of eluting the purified polyA$^+$ RNA, the RNA was reversed transcribed directly on the beads with Superscript III using the Oligo(dT)$_{25}$ as the reverse transcription primer. One-tenth of resulting cDNA was then pre-amplified using MyTaq Red Mix (Meridian Bioscience) with the 5′ adaptor and MYL9r primers (Supplementary table 2) for 30 cycles. One-twentieth of the pre-amplified produced was then analysed by quantitative PCR using GoTaq qPCR Master Mix with the 5′ adaptor and MYL9-372 (nested) primers. This strategy detects the cleavage site at position 324 in the MYL9 mRNA. The nested PCR products were Sanger sequenced to confirm detection of the correct cleavage site.

Analysis of the *TCONS_l2_00017631* locus on human chromosome 22

RNAseq and H3K4me4 ChIPseq datasets of human embryonic stem cells were obtained from the ENCODE portal[31] (https://www.encodeproject.org/). These were

aligned to human genome (GRCh38/hg38) and visualised in the UCSC Genome Browser.[32]

Western blotting for DROSHA and DICER knockdown

Jurkat cells were cultured in RPMI + 10% FCS. They were transduced with lentiviral shRNAs against DROSHA, DICER or an empty vector. After 3 days, the transduced cells (GFP^+) were sorted to purity and returned to culture for an additional 3 days to expand. The cells were then harvested, washed in cold PBS and lysed in RIPA buffer. The lysates were then analysed for DROSHA or DICER protein expression by Western blotting. Analysis of β-actin employed as a loading control. Separate gels were run to detect β-actin due to the difference in detection sensitivity compared with the detection of the RNase III enzymes. Lysates from 5×10^6 cells were loaded for the DROSHA and DICER blots, while lysates from 2×10^5 cells were loaded for the β-actin blots. The rabbit monoclonal antibodies to detect DROSHA (clone EPR12794) and DICER (clone EPR24104-105) were purchased from Abcam (Cambridge), while the rabbit monoclonal antibody to detect β-actin (clone 13E5) was purchased from Cell Signaling Technology (Danvers).

Cell cycle analysis

Cord blood $CD34^+$ cells were transduced with lentiviral shRNAs against DROSHA or DICER, or a GFP only control. After 3 days in culture, the GFP^+-transduced cells were sorted to purity. The cells were returned to culture for a further 5 days and then analysed for cell cycle status by fixing in 4% paraformaldehyde (in PBS) and staining with propidium iodide. The cells were then analysed for DNA content by flow cytometry. Cells in S or G2/M phase were considered proliferating.

Statistical analysis

Statistical analysis and graphical representation of datasets were performed using Prism v9.0 (GraphPad, San Diego, USA). Differences between groups were tested using a two-way ANOVA and Tukey's multiple comparisons analysis. Results were considered statistically significant at $P < 0.05$.

ACKNOWLEDGMENTS

This work was supported by grants and fellowships from the National Health and Medical Research Council (1117154, 1122384 and 1122395 to MMWC), Diabetes Australia Research Trust (Y20G-CHOM to MMWC), US Department of Defense (W81XWH-19-1-0728 to MMWC), The Ann Helene Toakley Charitable Endowment (to MMWC) and the Mater Foundation (to KJR). St. Vincent's Institute of Medical Research is supported by the Victorian State Government Operational Infrastructure Support and the Independent Research Institutes Infrastructure Support Scheme of the National Health and Medical Research Council. The Translational Research Institute is supported by a grant from the Australian Government.

CONFLICT OF INTEREST

The authors declare no conflict of interest.

AUTHOR CONTRIBUTIONS

Karen Gu: Conceptualization; Data curation; Formal analysis; Investigation; Methodology; Writing – original draft. **Carina Walpole:** Data curation; Formal analysis; Investigation; Methodology. **Shayarana Gooneratne:** Conceptualization; Data curation; Formal analysis; Investigation; Methodology. **Xin Liu:** Data curation; Formal analysis; Investigation; Methodology; Visualization. **Oscar L Haigh:** Investigation; Methodology. **Kristen J Radford:** Conceptualization; Funding acquisition; Resources; Supervision; Writing – review & editing. **Mark MW Chong:** Conceptualization; Data curation; Formal analysis; Funding acquisition; Resources; Supervision; Visualization; Writing – original draft; Writing – review & editing.

REFERENCES

1. Akashi K, Traver D, Miyamoto T, Weissman IL. A clonogenic common myeloid progenitor that gives rise to all myeloid lineages. *Nature* 2000; **404**: 193–197.
2. Kondo M, Weissman IL, Akashi K. Identification of clonogenic common lymphoid progenitors in mouse bone marrow. *Cell* 1997; **91**: 661–672.
3. Naik SH, Perié L, Swart E *et al*. Diverse and heritable lineage imprinting of early haematopoietic progenitors. *Nature* 2013; **496**: 229–232.
4. Johanson TM, Keown AA, Cmero M *et al*. DROSHA controls dendritic cell development by cleaving messenger RNAs encoding inhibitors of myelopoiesis. *Nat Immunol* 2015; **16**: 1134–1141.
5. Lee Y, Ahn C, Han J *et al*. The nuclear RNase III DROSHA initiates microRNA processing. *Nature* 2003; **425**: 415–419.
6. Yeo JH, Chong MM. Many routes to a micro RNA. *IUBMB Life* 2011; **63**: 972–978.
7. Johanson TM, Lew AM, Chong MM. MicroRNA-independent roles of the RNase III enzymes DROSHA and DICER. *Open Biol* 2013; **3**: 130144.
8. Knuckles P, Vogt MA, Lugert S *et al*. DROSHA regulates neurogenesis by controlling neurogenin 2 expression independent of microRNAs. *Nat Neurosci* 2012; **15**: 962–969.
9. Karginov FV, Cheloufi S, Chong MM, Stark A, Smith AD, Hannon GJ. Diverse endonucleolytic cleavage sites in the mammalian transcriptome depend upon microRNAs, DROSHA, and additional nucleases. *Mol Cell* 2010; **38**: 781–788.
10. Han J, Pedersen JS, Kwon SC *et al*. Posttranscriptional crossregulation between DROSHA and DGCR8. *Cell* 2009; **136**: 75–84.
11. Triboulet R, Chang HM, Lapierre RJ, Gregory RI. Post-transcriptional control of DGCR8 expression by the Microprocessor. *RNA* 2009; **15**: 1005–1011.

12. de Rie D, Abugessaisa I, Alam T *et al*. An integrated expression atlas of miRNAs and their promoters in human and mouse. *Nat Biotechnol* 2017; **35**: 872–878.
13. Gruber AR, Lorenz R, Bernhart SH, Neubock R, Hofacker IL. The Vienna RNA websuite. *Nucleic Acids Res* 2008; **36**: W70–74.
14. Gu K, Mok L, Chong MMW. Regulating gene expression in animals through RNA endonucleolytic cleavage. *Heliyon* 2018; **4**: e00908.
15. Wu H, Xu H, Miraglia LJ, Crooke ST. Human RNase III is a 160-kDa protein involved in preribosomal RNA processing. *J Biol Chem* 2000; **275**: 36957–36965.
16. Chong MM, Rasmussen JP, Rudensky AY, Littman DR. The RNAseIII enzyme DROSHA is critical in T cells for preventing lethal inflammatory disease. *J Exp Med* 2008; **205**: 2005–2017.
17. Oskowitz AZ, Penfornis P, Tucker A, Prockop DJ, Pochampally R. DROSHA regulates hMSCs cell cycle progression through a miRNA independent mechanism. *Int J Biochem Cell Biol* 2011; **43**: 1563–1572.
18. Havens MA, Reich AA, Hastings ML. DROSHA promotes splicing of a pre-microRNA-like alternative exon. *PLoS Genet* 2014; **10**: e1004312.
19. Lee D, Nam JW, Shin C. DROSHA targets its own transcript to modulate alternative splicing. *RNA* 2017; **23**: 1035–1047.
20. Francia S, Michelini F, Saxena A *et al*. Site-specific DICER and DROSHA RNA products control the DNA-damage response. *Nature* 2012; **488**: 231–235.
21. Dueck A, Ziegler C, Eichner A, Berezikov E, Meister G. microRNAs associated with the different human Argonaute proteins. *Nucleic Acids Res* 2012; **40**: 9850–9862.
22. Wei W, Ba Z, Gao M *et al*. A role for small RNAs in DNA double-strand break repair. *Cell* 2012; **149**: 101–112.
23. Cho SH, Ko JJ, Kim JO *et al*. 3′-UTR polymorphisms in the miRNA machinery genes DROSHA, DICER1, RAN, and XPO5 are associated with colorectal cancer risk in a Korean population. *PLoS One* 2015; **10**: e0131125.
24. Jiang X, Wooderchak-Donahue WL, McDonald J *et al*. Inactivating mutations in DROSHA mediate vascular abnormalities similar to hereditary hemorrhagic telangiectasia. *Sci Signal* 2018; **11**: eaan6831.
25. Rakheja D, Chen KS, Liu Y *et al*. Somatic mutations in DROSHA and DICER1 impair microRNA biogenesis through distinct mechanisms in Wilms tumours. *Nat Commun* 2014; **2**: 4802.
26. Torrezan GT, Ferreira EN, Nakahata AM *et al*. Recurrent somatic mutation in DROSHA induces microRNA profile changes in Wilms tumour. *Nat Commun* 2014; **5**: 4039.
27. Zhang Z, Zhang G, Kong C *et al*. EIF2C, DICER, and DROSHA are up-regulated along tumor progression and associated with poor prognosis in bladder carcinoma. *Tumour Biol* 2015; **36**: 5071–5079.
28. Manel N, Hogstad B, Wang Y, Levy DE, Unutmaz D, Littman DR. A cryptic sensor for HIV-1 activates antiviral innate immunity in dendritic cells. *Nature* 2010; **467**: 214–217.
29. Pearson FE, Chang K, Minoda Y *et al*. Activation of human CD141$^+$ and CD1c$^+$ dendritic cells *in vivo* with combined TLR3 and TLR7/8 ligation. *Immunol Cell Biol* 2018; **96**: 390–400.
30. Balan S, Ollion V, Colletti N *et al*. Human XCR1$^+$ dendritic cells derived *in vitro* from CD34$^+$ progenitors closely resemble blood dendritic cells, including their adjuvant responsiveness, contrary to monocyte-derived dendritic cells. *J Immunol* 2014; **193**: 1622–1635.
31. Davis CA, Hitz BC, Sloan CA *et al*. The encyclopedia of DNA elements (ENCODE): data portal update. *Nucleic Acids Res* 2018; **46**: D794–D801.
32. Kent WJ, Sugnet CW, Furey TS *et al*. The human genome browser at UCSC. *Genome Res* 2002; **12**: 996–1006.

Supporting Information

Additional supporting information may be found online in the Supporting Information section at the end of the article.